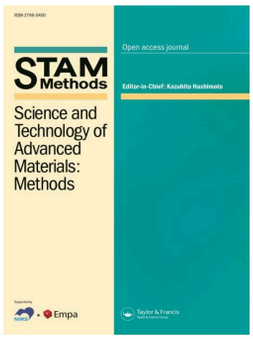

Taylor & Francis
Taylor & Francis Group

Science and Technology of Advanced Materials: Methods

ISSN: 2766-0400 (Online) Journal homepage: www.tandfonline.com/journals/tstm20

Efficient discovery of large magnetic anisotropy with thermodynamically stable materials via multi-objective Bayesian optimization

Kohei Nakamura, Daigo Furuya, Yoshio Miura, Takahiro Yamazaki, Alexandre Lira Foggiatto, Yuma Iwasaki & Masato Kotsugi

To cite this article: Kohei Nakamura, Daigo Furuya, Yoshio Miura, Takahiro Yamazaki, Alexandre Lira Foggiatto, Yuma Iwasaki & Masato Kotsugi (2025) Efficient discovery of large magnetic anisotropy with thermodynamically stable materials via multi-objective Bayesian optimization, Science and Technology of Advanced Materials: Methods, 5:1, 2485025, DOI: 10.1080/27660400.2025.2485025

To link to this article: https://doi.org/10.1080/27660400.2025.2485025

SCIENCE AND TECHNOLOGY OF ADVANCED MATERIALS: METHODS
2025, VOL. 5, NO. 1, 2485025
https://doi.org/10.1080/27660400.2025.2485025

Efficient discovery of large magnetic anisotropy with thermodynamically stable materials via multi-objective Bayesian optimization

Kohei Nakamura[a], Daigo Furuya[a], Yoshio Miura[b], Takahiro Yamazaki[a], Alexandre Lira Foggiatto[a], Yuma Iwasaki[c] and Masato Kotsugi[a]

[a]Faculty of Advanced Engineering, Tokyo University of Science, Tokyo, Japan; [b]Research Center for Magnetic and Spintronic Materials (CMSM), National Institute for Materials Science (NIMS), Ibaraki, Japan; [c]Center for Basic Research on Materials (CBRM), National Institute for Materials Science (NIMS), Ibaraki, Japan

ABSTRACT

This study presents an efficient magnetic material exploring method with large magnetocrystalline anisotropy (MCA) and thermodynamic stability by combining multi-objective Bayesian optimization (MBO) with first-principles calculations. Focusing on six-layer tetragonal ordered alloys of rare-earth-free elements (Fe, Co, Ni, Cu), our approach optimizes material properties and process conditions within high-dimensional spaces. Explanatory variables derived from elemental and structural information were employed to enhance Bayesian optimization. Utilizing Gaussian process regression and dimensionality-reduced descriptors, we achieved efficient and robust exploration for precomputed dataset. As a result, MBO efficiently suggested the following three materials – Fe/Fe/Fe/Ni/Fe/Ni, Fe/Co/Fe/Co/Fe/Ni, and Fe/Co/Co/Fe/Ni/Ni – that exhibit thermodynamic stability while demonstrating an MCA value up to four times larger than that of $L1_0$-FeNi. The developed methodology accelerates material discovery and reduces resource demands, offering a scalable materials solution for optimizing functionality and process conditions across diverse material systems.

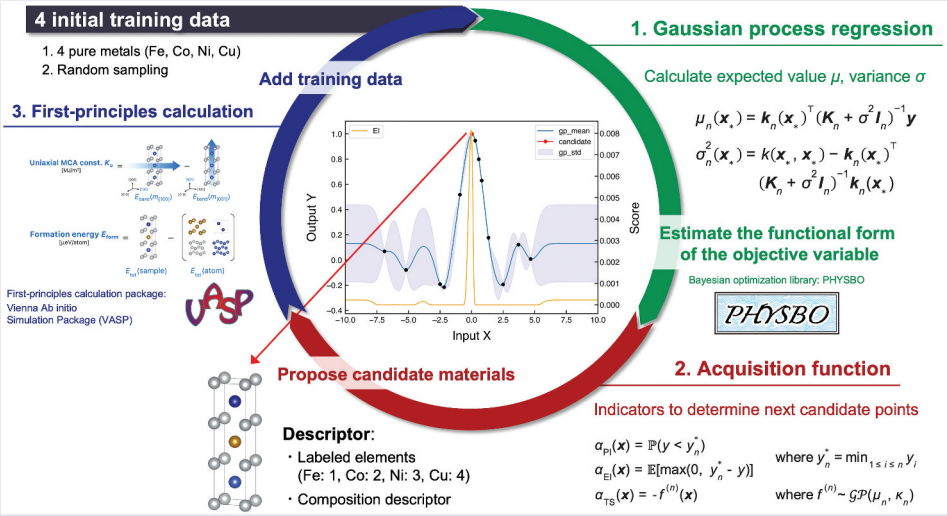

IMPACT STATEMENT

This study accelerates advanced magnetic materials discovery by integrating multi-objective Bayesian optimization and first-principles calculations, uncovering rare-earth-free alloys with exceptional magnetocrystalline anisotropy and thermodynamic stability, enabling scalable materials development.

ARTICLE HISTORY
Received 3 December 2024
Revised 14 March 2025
Accepted 24 March 2025

KEYWORDS
Magnetocrystalline anisotropy; formation energy; bayesian optimization; multi-objective optimization; first-principles calculation; materials informatics; magnetic materials

1. Introduction

Advanced magnetic materials with large magnetocrystalline anisotropy (MCA) are critically important for the realization of next-generation devices. In spintronics applications, MCA dictates increasing device medium density, data retention capabilities, and even the power consumption and speed of writing processes [1,2]. Large MCA arises from a complex

CONTACT Masato Kotsugi kotsugi@rs.tus.ac.jp Faculty of Advanced Engineering, Tokyo University of Science, 6-3-1, Niijuku, Katsushika, Tokyo 125-8585, Japan

Supplemental data for this article can be accessed online at https://doi.org/10.1080/27660400.2025.2485025

interplay related to crystallographic symmetry in multilayer, types of constituting elements, the number of layers, stacking sequences, and distortions [3–7]. Thereby, precise design of these multilayer structure is essential to improve MCA. In film deposition processes, the thermodynamic stability of candidate materials based on their formation energies should be analyzed comprehensively. This necessitates the simultaneous optimization of the functional property of MCA and the processing conditions of the multilayers.

However, establishing a correlation between MCA and formation energy is challenging, and their relationship remains unclear. In addition, the vast number of possible multilayer configurations leads to a combinatorial explosion, rendering experimental structural evaluations and MCA measurements impractical. Against this backdrop, exploring materials in a high-dimensional space that encompasses critical functions like MCA and processing conditions like formation energy has been exceedingly difficult through both theoretical calculations and experimental approaches.

Recently, materials informatics (MI), which integrates materials science with data science, has garnered significant attention. MI is a data-driven approach that employs artificial intelligence and machine learning to analyze materials data, aiding in the discovery of unknown materials and informed decision-making in experimental development. It holds great promise for the creation of innovative materials and the acceleration of materials development and is considered highly effective for optimizing the complex material parameters mentioned above.

In this study, we focus on Bayesian optimization, a prominent method in data science, to simultaneously optimize the functions and processes of magnetic materials. Bayesian optimization is a leading example of black-box function optimization techniques using Gaussian process, offering significant advantages in optimizing material functions and discovering promising materials from an extensive search space [8]. It constructs a statistical model for functions where the relationship between inputs and outputs is unknown, proposes the next candidate based on this model, and updates the model sequentially with new data. By repeating this process, it becomes possible to obtain optimal solutions with a minimal number of trials, even for functions with high evaluation costs. Bayesian optimization has been widely applied in the development of various materials – including magnetic materials, thermoelectric materials, catalytic materials, and semiconductor materials – and has led to the discovery of new materials unattainable by conventional manual exploration methods [9–17].

Moreover, multi-objective Bayesian optimization enables the simultaneous optimization of multiple objective variables and is particularly effective when these variables are in a trade-off relationship [18,19]. This method also employs Gaussian process regression to efficiently explore the solution space, identifying Pareto-optimal solutions that are not dominated by any other solutions and forming a Pareto front from these solutions. By introducing diversity metrics, multi-objective Bayesian optimization performs comprehensive optimization while efficiently exploring and expanding the Pareto front. This approach offers advantages such as efficient exploration, consideration of uncertainties and visualization of trade-offs. Therefore, multi-objective Bayesian optimization is an effective strategy for complex optimization problems and is expected to enable efficient material discovery in high-dimensional spaces that include critical magnetic properties like magnetocrystalline anisotropy (MCA) and process parameters like formation energy. Including systems with positive Formation Energy enables a more comprehensive exploration of material properties and potential experimental stabilization strategies. Utilizing this method allows us to select the promising materials with thermodynamic stability and MCA properties before experiment, thereby accelerating the overall development process while reducing human and time resources.

Specifically, we have developed a method that combines first-principles calculations with Bayesian optimization to efficiently explore promising advanced magnetic materials from a vast material space. By leveraging multi-objective Bayesian optimization, we simultaneously optimized for large MCA and stable multilayer structures. In our development process, we performed optimization on various types of initial training data to achieve robust exploration, determining the optimal acquisition functions and designing descriptors accordingly.

2. Methods

Figure 1 shows the workflow of this study. This study is based on $L1_0$-FeNi and $L1_0$-FeCo, which are rare-earth-free alloys with large MCA, and targets a six-layer periodic tetragonal ordered alloy composed of four rare-earth-free elements (Fe, Co, Ni, and Cu). We used the Vienna Ab initio Simulation Package (VASP) as the ab initio package, which allows the use of plane-wave basis and pseudopotential methods [20–22]. We also used SHRY [23], pymatgen [24] to generate the input files for VASP. The calculations used the generalized gradient approximation (GGA) proposed by Perdew, Burke, and Ernzerhof (PBE) for the exchange-correlation functional [25]. The nucleus and core electrons are described by Projector Augmented Wave (PAW) potentials [26], and the wavefunction of the

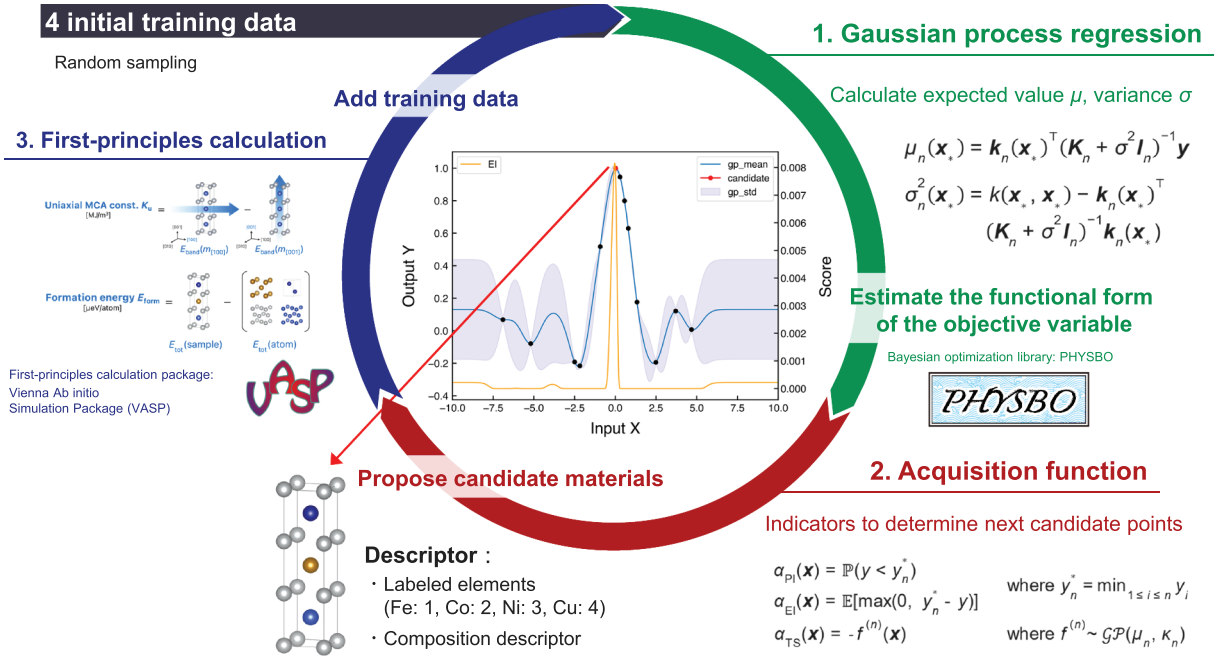

Figure 1. Workflow for autonomous search for large-magnetic anisotropy materials combining Bayesian optimization and first-principles calculations. Bayesian optimization is performed on four types of initial training data to determine promising candidate materials. The proposed candidate materials are calculated using first-principles calculations and added to the training data, and the process is repeated until the optimal solution is obtained.

valence electron is expanded in a plane-wave basis with a cutoff energy of 369.3 eV. The number of *k*-points was set to 12 × 12 × 6 for structural relaxation and 24 × 24 × 9 for MCA calculation. The Monkhorst-Pack method was used for *k*-point sampling [27], and the tetrahedral method of Blöchl correction was used for *k*-space integration, which allows accurate integration of *k*-points in the Brillouin Zone [28]. In the structural relaxation, the tetragonal crystal structure was used as the unit cell, and the atomic positions, the in-plane lattice parameter *a* and out-of-plane lattice parameter *c* were optimized so that the total energy was less than 10^{-6} eV. MCA calculations were performed using force theorem [29,30], and the convergence condition was set to a total energy of less than 10^{-6} eV. MCA energy E_{MCA} was defined as the difference between the energy eigenvalues in the [100] and [001] directions, and E_{MCA} per unit cell volume as K_u, so that E_{MCA}, K_u >0 at perpendicular magnetic anisotropy. Formation energy E_{form} was calculated by subtracting the total energy of the stable crystal structure of each element from the total energy of the ordered alloy. The calculations were performed in parallel (AMD Ryzen™ Threadripper™ 1950X 16-Core Processor, Number of cores: 16, Memory size: 64 GB) using 13 processes, and the total calculation time for all 430 candidate materials was approximately 3 months.

We here focus on two types of techniques: simple Bayesian optimization for K_u and multi-objective Bayesian optimization for the formation energy E_{form} and K_u. We employed PHYSBO [31,32] as a Python library to implement Bayesian optimization. The number of initial training data was set to 4 according to the elemental species in use. The acquisition functions were Thompson Sampling (TS), Expected Improvement (EI), and Probability of Improvement (PI) for Bayesian optimization [33–35], and Thompson Sampling (TS), Expected Hyper-Volume Improvement (EHVI), and Hypervolume-based Probability of Improvement (HVPI) were used for multi-objective Bayesian optimization [33,36]. Hyperparameters for Bayesian optimization was relearned every iteration to adapt dynamically to data distribution changes, ensuring model robustness and accuracy. We defined simple discrete-valued features as explanatory variables used in Bayesian optimization, first for the four elements (Fe, Co, Ni, and Cu) entering each layer by label encoding: Fe = {1}, Co = {2}, Ni = {3}, and Cu = {4}. Then, the stacking structure was represented by a 6-dimensional array since the periodicity of the layers is 6 layers. In previous studies [13], Bayesian optimization was performed using only elements labeled as explanatory variables, but this approach may incorrectly learn information about elements that should be treated as nominal measures as ordinal measures. We believe that more efficient Bayesian optimization can be achieved by defining element-related information as explanatory variables, rather than defining explanatory variables only for label encoding, even in light of future expansion of the materials search space by increasing the number of elements used.

We generated 290 compositional descriptors based solely on periodic table information such as atomic number and atomic weight of inorganic materials using XenonPy [37]. We selected 53 descriptors from the generated compositional descriptors and combined them with a 6-dimensional array showing the stacking structure to define a 59-dimensional descriptor. The 53 descriptors were selected from among the basic physical property values that can be calculated using only atomic number and composition, with the exception of descriptors with constant values. We also used an autoencoder to reduce the dimensionality of descriptors since the explanatory variables in Bayesian optimization function properly in 20 dimensions or less [18,38]. Information from the 59-dimensional descriptors was compressed in the middle layer of a neural network with the same input and output layers, creating a new 20-dimensional descriptor. Keras/TensorFlow [39] was used as the Python library, the activation function was set to the tanh function, the iteration time to 300, and the hidden layer size to 20. Normalization was applied to all descriptors such that the minimum is 0 and the maximum is 1, preventing dimensionality reduction inaccuracy due to scale differences. More details of difference of objective variables scaling are given in supplementary materials (S1). Mean Squared Error (MSE) was 0.00876208 and Root Mean Squared Error (RMSE) was 0.0936059. Figure S2 illustrates the MSE convergence over 300 epochs, confirming the effective training of the autoencoder. The maximum error observed was 0.27028, which demonstrates the reliability of the dimensionality reduction process. More details of MSE convergence are given in supplementary materials (S2).

3. Results and discussion

In Bayesian optimization, Initial training data is given either by artificial sampling or random sampling. Thus, we investigated the search performance of Bayesian optimization on 100 sets of randomly sampled initial training data in order to develop a robust search method that is independent of the type of initial training data. Figure 2 presents single-objective optimization results with three types of descriptors on 100 randomly selected sets of initial training data. To determine the optimal acquisition function and descriptors, acquisition functions were TS, EI, and PI. Descriptors were descriptors labeled Fe = {1}, Co = {2}, Ni = {3}, and Cu = {4} for each element (6 dimensions), descriptors with composition descriptors added to the labeled elements (59 dimensions), and descriptors created by autoencoder from the labeled elements and composition descriptors (20 dimensions). Figure 2 (a)–(c) shows the history of maximum K_u by the number of iterations. It is clear that regardless of the type of initial training data, it is possible to find material with maximum K_u in less than 30% of the total number of iterations for all descriptors and acquisition functions. Figure 2 (d)–(f) shows the number of appearances of materials with the top two K_u values for each number of trials. Figure 2 (d) and (f) show that the materials with the top two K_u are found by about 50 iterations when only elements labeled with the descriptors and when both labeled elements and compositional descriptors are dimensionally reduced using an autoencoder. Figure 2 (e) shows that the material with the largest K_u is found by around 100 iterations, and the material with the second largest K_u is found after that.

Table 1 shows the average number of iterations in which the top two materials with the largest K_u are found for 100 sets of initial training data. It can be seen that Bayesian optimization clearly finds materials with large K_u in a smaller number of iterations compared to the random sampling results. The most efficient descriptors for material search were for the labeled elements only. However, this result may be the reflection of mislearning due to the labeling of Cu = {4}, since many of the candidate materials in this study that showed large K_u contained a lot of Cu. On the other hand, when the labeled elements and composition descriptors are dimension-reduced by the autoencoder, the search performance is equivalent to that of the labeled elements alone. This descriptor avoids mislearning labels as an ordinal scale rather than a nominal scale. The composition descriptor can be calculated only with information from the periodic table. Therefore, even if the material search space is expanded in the future, efficient material search in Bayesian optimization can be realized by using the descriptor generated by dimensionality reduction of the labeled elements and the composition descriptor with the autoencoder. In this study, we developed a new 20-dimensional descriptor by autoencoding the 6-dimensional array representing the stacking structure and the 53-dimensional compositional descriptor calculated from the composition, and used it as an explanatory variable for Bayesian optimization. Also, it was found that the Bayesian optimization using EI as the acquisition function found the material with the largest K_u in about 10% of the total number of iterations. This means that large magnetic anisotropy materials can be found in about 10 days of the total calculation time, which is about 3 months for all candidate materials. Therefore, even with limited computational resources at the laboratory level, this research model can be expected to speed up the material search by up to 9 times.

Figure 3 shows the relationship between K_u and various material properties for all candidate materials obtained through autonomous search by a combination of first-principles calculations and Bayesian optimization. First, as shown in Figure 3 (a)

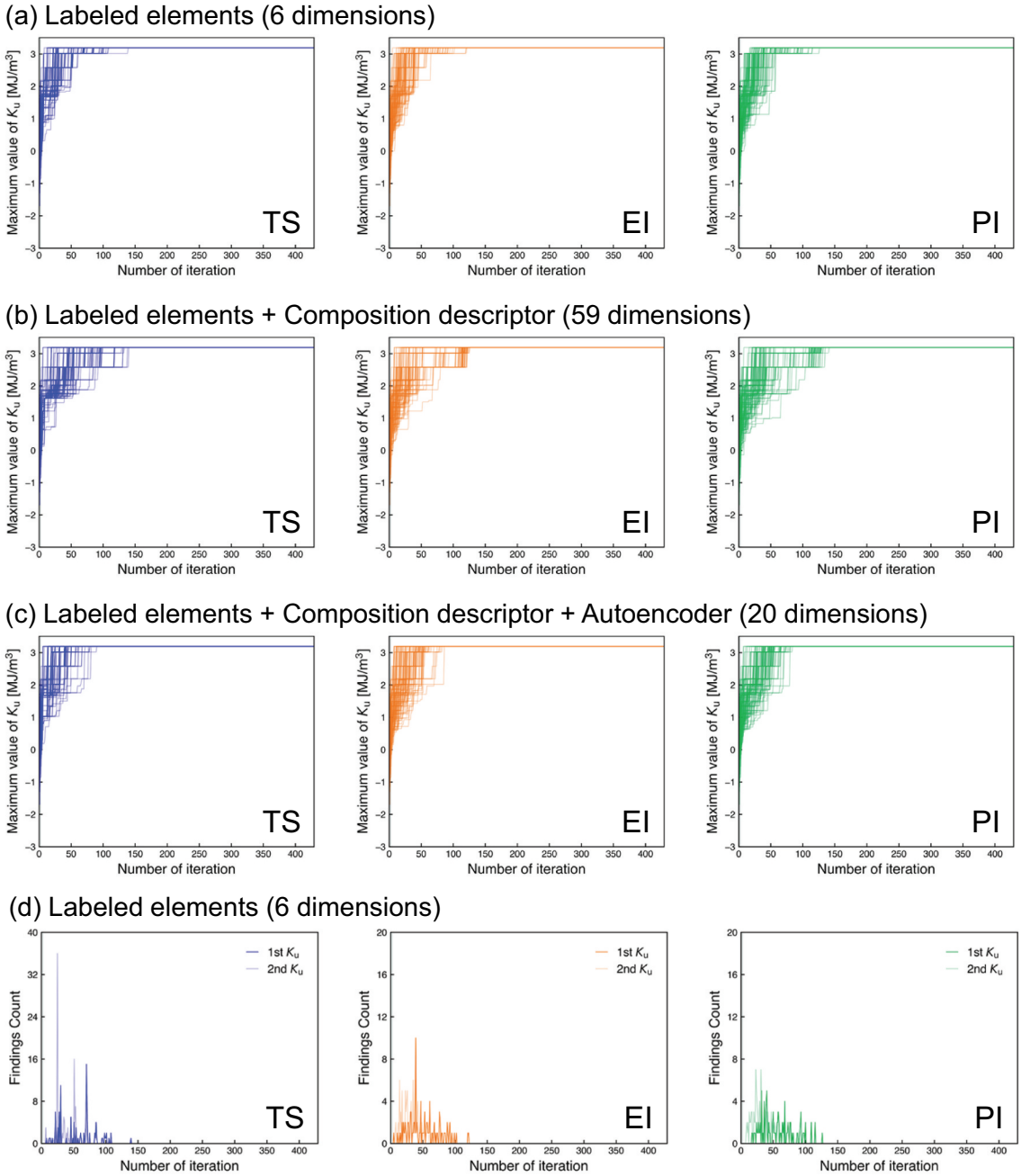

Figure 2. (a–c) Bayesian optimization results for 100 sets of initial training data. (d–f) Number of appearances of the top two materials with Ku. Descriptors are set to (a, d) labeled elements, (b, e) labeled elements and composition descriptor, (c, f) labeled elements, composition descriptor and autoencoder. Acquisition functions were set to TS, EI and PI. The gray band represents the initial training data.

and (b), K_u varies greatly depending on the crystal structure; in Figure 3 (a), as in the previous study [13], materials with K_u = >1.00 MJ/m^3 exhibit the fcc structure. On the other hand, most of the materials showing the bcc structure are below K_u = 1.00 MJ/m^3. By excluding bcc materials from the candidate materials in advance, the search efficiency of Bayesian optimization can be improved, and this result will serve as a guideline for future extended material search space. Figure 3 (b) shows that K_u varies with unit cell volume, and the variation is discontinuous. There are many materials with the same composition but different elemental stacking order because only four elements make up the materials in this study. Since these materials have similar unit cell volumes, it is considered that K_u varies discontinuously with unit cell volume, as shown in Figure 3 (b).

Figure 3 (c) and (d) show that K_u is independent of the formation energy and magnetic moment. Formation energies that are negative indicate that the material is thermodynamically stable. This is a very important material property in view of the

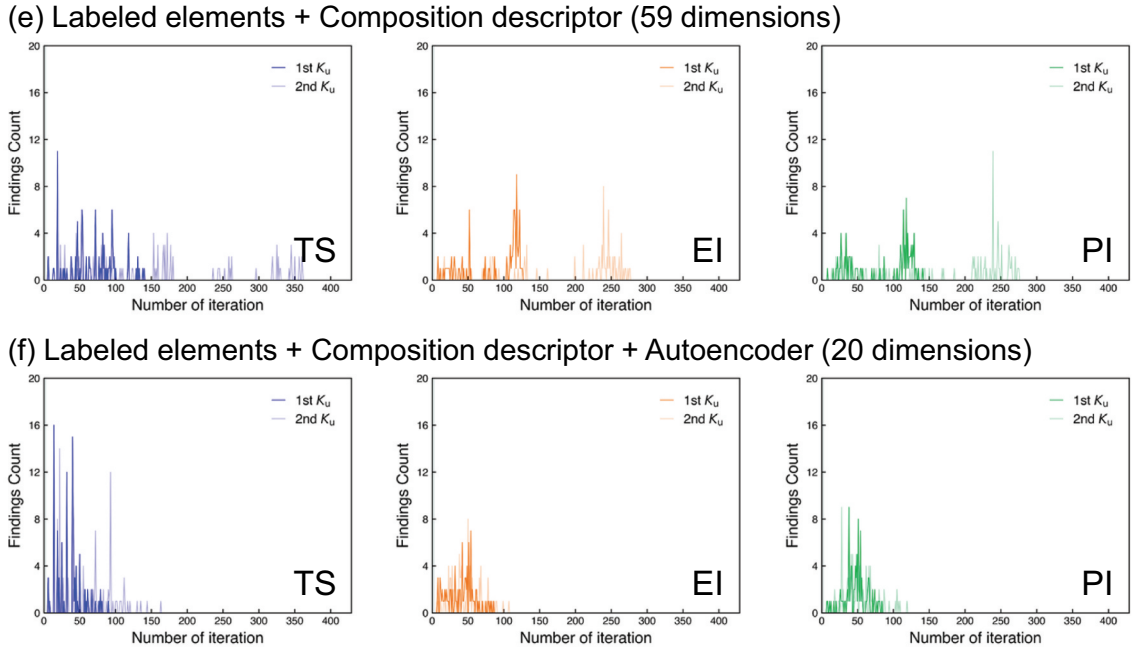

Figure 2. (Continued).

Table 1. Dependence on descriptors of the average number of iterations that the top two K_u materials are found. Random sampling results are shown for reference.

Method	Acquisition function	Average number of iterations
Random sampling	–	206.2 ± 21.4
Bayesian optimization + Labeled elements	TS	46.8 ± 21.5
	EI	41.2 ± 13.5
	PI	44.0 ± 13.1
Bayesian optimization + Labeled elements + Composition descriptor	TS	123.4 ± 21.2
	EI	133.0 ± 24.9
	PI	129.4 ± 25.5
Bayesian optimization + Labeled elements + Composition descriptor + Autoencoder	TS	51.1 ± 18.6
	EI	43.9 ± 14.4
	PI	49.7 ± 15.8

experimental fabrication of materials explored by Bayesian optimization. However, as shown in Figure 3 (c), there is no strong correlation between K_u and formation energy, making it very difficult to search for materials with small formation energy but large K_u. Therefore, we believe that the search for large magnetic anisotropy materials that can be experimentally fabricated can be achieved by applying multi-objective Bayesian optimization, which can optimize multiple objective variables, rather than Bayesian optimization, which optimizes a single objective variable.

Figure 3 (e) shows K_u and the orbital magnetic moment anisotropy Δm_{orb}, where Δm_{orb} is the difference between the orbital magnetic moment m_{orb} oriented in the [001] and [100] directions. K_u and Δm_{orb} have a strong linear correlation, and Pearson's product-moment correlation coefficient r was calculated to be $r = 0.769$. The strong linear correlation between K_u and Δm_{orb} can be attributed to the fact that most of the candidate materials follow Bruno's model [40–42]. There is no definitive formula that connects material composition and magnetic anisotropy because K_u is determined through a complex relationship among constituent elements, crystal structure, electronic state, and other factors. However, as shown in Figure 3 (e), we can see a strong correlation between K_u and Δm_{orb}, suggesting that it is possible to find a descriptor that can represent K_u by combining other material properties based on Δm_{orb}.

Figure 4 focuses on multi-objective optimization outcomes. Figure 4 shows the history of dominant regions estimated from the Pareto front when multi-objective Bayesian optimization was performed on 100

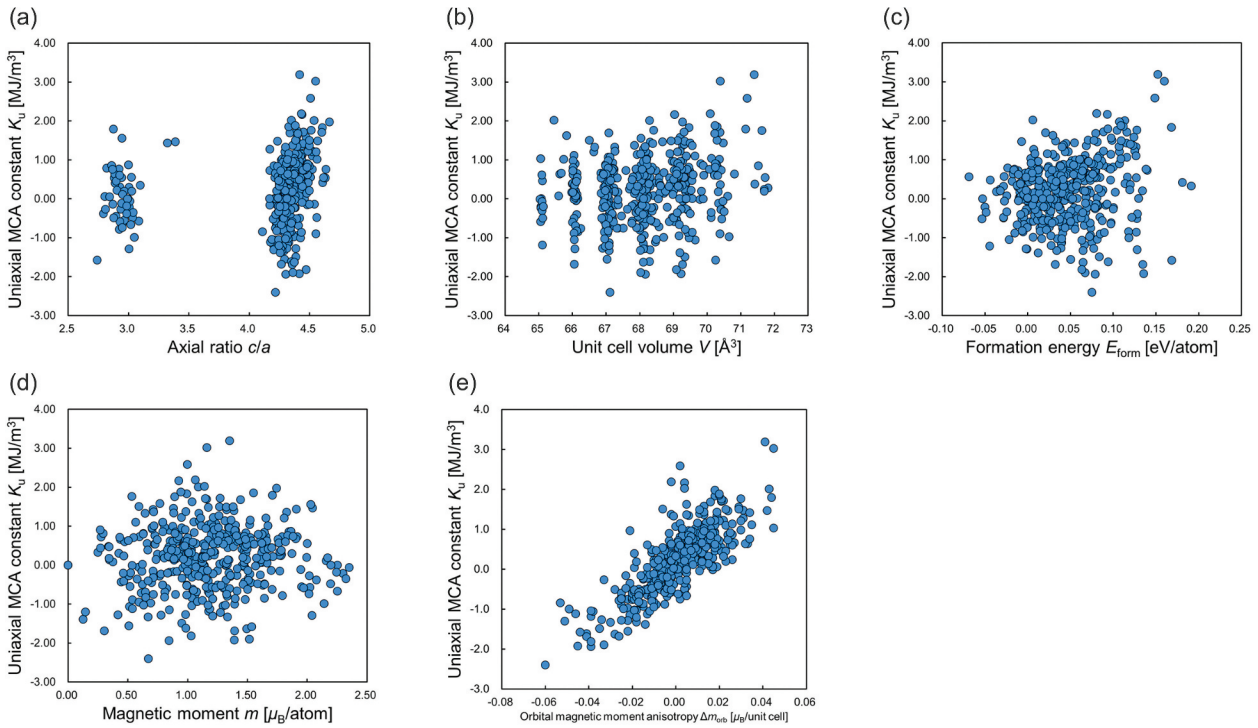

Figure 3. First principles calculation results for all 430 candidate materials. The relationship between the magnetocrystalline anisotropy energy K_u and various material properties are shown. (a) axial ratio c/a vs K_u, (b) unit cell volume V vs K_u, (c) formation energy E_{form} vs K_u, (d) magnetic moment m vs K_u, (e) orbital magnetic moment anisotropy Δm_{orb} vs K_u.

randomly selected sets of initial training data. The number of iterations for multi-objective Bayesian optimization was 100, about 25% of iterations of all materials. The dominated region for the entire dataset is 1.474, serving as a baseline for evaluating optimization results. The objective variables were the formation energy E_{form} and the magnetocrystalline anisotropy energy K_u, and the acquisition functions were TS, EHVI, and HVPI. Descriptors were newly generated by autoencoding the labeled elemental and compositional descriptors to reduce their dimensionality to 20 dimensions. Table 2 shows the average volume of the dominant regions finally obtained by multi-objective Bayesian optimization. It can be seen that the acquisition function as HVPI produced a smaller dominant region than the random sampling. This is considered to be because the search area was biased toward searching for material that does not contribute to expanding the dominant region. HVPI's prioritization of high-uncertainty regions limit Pareto front expansion, resulting in smaller dominated regions. More details of search result of HVPI are given in supplementary materials (S3).

On the other hand, when the acquisition functions were TS and EHVI, it is clear that the model succeeded in generating larger dominant regions than random sampling. The multi-objective Bayesian optimization with TS, EHVI was able to search for a variety of Pareto optimal solutions that contribute to the expansion of the dominant region regardless of the type of initial training data, which may indicate the robustness of the search model developed in this study.

Figure 5 shows the results of the search for large magnetic anisotropy materials by multi-objective Bayesian optimization. The number of iterations of the multi-objective Bayesian optimization is 100, which is about 25% of iterations of all materials, and the acquisition function is EHVI. As shown in Figure 5, the promising materials in this study are thermodynamically stable and exhibit large MCA. The known material, $L1_0$-FeNi, exhibits the smallest formation energy within the search space of this study, indicating that it is a very thermodynamically stable material. However, focusing on MCA, it can be seen that a number of new materials with MCA several times larger than that of $L1_0$-FeNi were efficiently discovered even with about 25% of iterations of all materials. These materials represent computational candidates suggested through Bayesian optimization applied to a precomputed dataset. The three new materials illustrated in Figure 5, Fe/Fe/Ni/Fe/Ni, Fe/Co/Fe/Co/Fe/Ni, and Fe/Co/Co/Fe/Ni/Ni, have slightly larger formation energies compared to $L1_0$-FeNi, but their values are zero or negative. So, we have discovered new materials that exhibit up to four times larger K_u than $L1_0$-FeNi with achieving thermodynamic stability. Especially, Fe/Co/Fe/Co/Fe/Ni is a bct structure with an axial ratio of $c/a = 3.32$, which is a structure in which Ni is substituted for a part of $B2$-FeCo. It is known that the axial ratio of the most stable

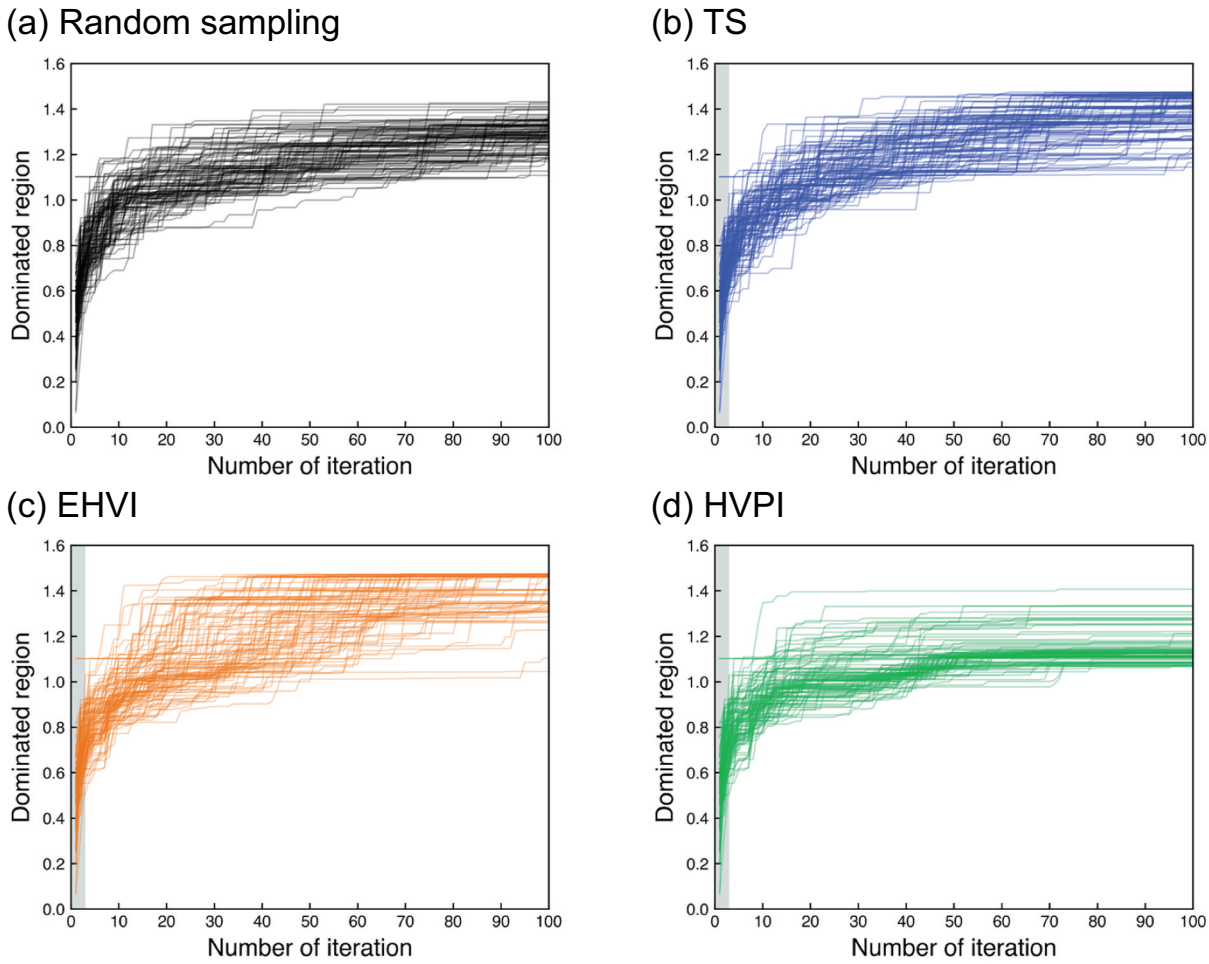

Figure 4. History of dominant regions during multi-objective Bayesian optimization on 100 sets of initial training data. (a) Random sampling, acquisition functions were set to (b) TS, (c) EHVI, and (d) HVPI. The number of iterations was 100, about 25% of the total number of iterations. The gray band represents the initial training data. The dominated region for the entire dataset is 1.474, serving as a baseline for evaluating optimization results.

Table 2. Dependence of the average dominated region on the acquisition function in multi-objective Bayesian optimization with 100 sets of initial training data.

Method	Acquisition function	Average dominated region
Random sampling	-	1.293 ± 0.067
Multi-objective	TS	1.383 ± 0.086
Bayesian optimization	EHVI	1.421 ± 0.082
	HVPI	1.145 ± 0.070

The acquisition functions were TS, EHVI, and HVPI. The dominated region for the entire dataset is 1.474, serving as a baseline for evaluating optimization results.

structure in $B2$-FeCo is $c/a = 1.0$, so that uniaxial magnetocrystalline anisotropy does not occur, but by distorting the crystal structure to a bct structure with $c/a = 1.25$, a giant magnetocrystalline anisotropy ($K_u = 6.0$ MJ/m^3) can be obtained [43–46]. Thus, improvement of K_u has been studied by epitaxial growth on a buffer layer with a bct structure and addition of a third element such as C or N to give crystal distortion to $B2$-FeCo [47,48]. Meanwhile, Fe/Co/Fe/Co/Fe/Ni has a bct structure as the most stable structure, so it is expected that Fe/Co/Fe/Co/Fe/Ni, which spontaneously shows large K_u, can be fabricated by selecting a buffer layer with an appropriate bct structure without the addition of a third element. In addition, it is expected to exhibit larger K_u as in $B2$-FeCo by controlling the in-plane lattice constant of the buffer layer and providing crystal distortion. It is very difficult to explore materials manually while taking into account all aspects of crystal structure, thermodynamic stability, and material properties, but by using the method in this study, we were able to explore novel materials without human preconceptions.

The results of this study demonstrate efficient material search by utilizing multi-objective Bayesian optimization to add formation energy related to process conditions to MCA. This is expected to enable efficient

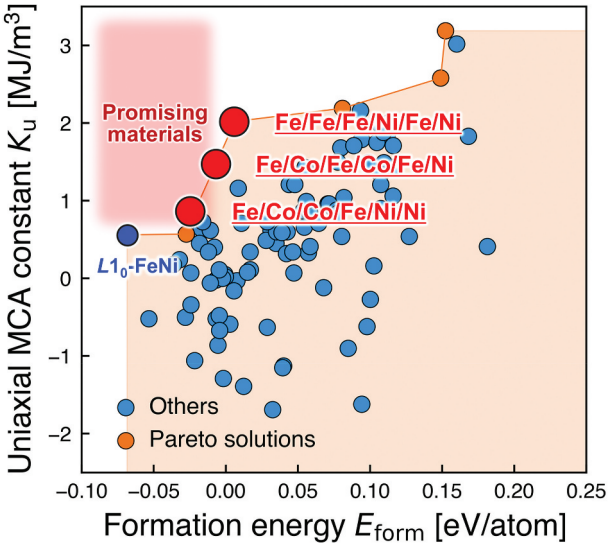

Figure 5. Results of multi-objective Bayesian optimization with EHVI as the acquisition function. The orange region represents the dominated region by the pareto solution. Three new promising materials, Fe/Fe/Fe/Ni/Fe/Ni, Fe/Co/Fe/Co/Fe/Co/Fe/Ni, and Fe/Co/Co/Fe/Ni/Fe/Ni/Ni, were found to be thermodynamically stable beyond the K_u of the previously known material, $L1_0$-FeNi.

virtual screening of novel materials that are realistically fabricable as well as highly functional, leading to faster material development. In the future, the three new materials proposed in this study will be fabricated by the monoatomic alternating stacking method, and their magnetic functions will be analyzed in detail using synchrotron radiation. Moreover, we will expand the material search space by increasing the number of elemental species to search for materials that are thermodynamically stable and exhibit larger MCA, and we will also search for new materials by optimizing various functions and process conditions other than MCA.

4. Conclusions

In this study, we attempted to develop an efficient material exploration method in a high-dimensional space that incorporates both MCA and process-related conditions such as formation energy, by combining multi-objective Bayesian optimization with first-principles calculations. To construct a robust exploration model, we investigated exploration efficiency by varying acquisition functions and explanatory variables against 100 sets of initial training data. Using descriptors representing the stacking structure and composition, along with newly generated descriptors via dimensionality reduction and employing EI acquisition function, we found that the material with the largest MCA could be discovered in approximately 10% of the total iterations. Furthermore, in multi-objective Bayesian optimization, where the acquisition function and designed explanatory variables were varied, we discovered that using EHVI as the acquisition function allowed the exploration of diverse Pareto optimal solutions, which contributed to the expansion of the dominated region in approximately 25% of the total iterations, independent of the initial training data. Through multi-objective Bayesian optimization, we discovered three new materials – Fe/Fe/Fe/Ni/Fe/Ni, Fe/Co/Fe/Co/Fe/Ni, and Fe/Co/Co/Fe/Ni/Ni – that exhibit MCA values up to 4 times higher than $L1_0$-FeNi with maintaining thermodynamic stability. These results are expected to accelerate materials development suitable optimization of both functionality and process, open a possibility for practical materials. Going forward, experimental fabrication of the proposed materials and detailed analysis using synchrotron radiation are expected. The synergy between theoretical materials exploration and experimental synthesis is poised to drive significant advancements in the development of cutting-edge new materials.

Acknowledgements

We thank to Dr. Igarashi, Dr. Sakuraba, Prof. Shimizu, Prof. Ando and Prof. Ono for useful discussions. We gratefully acknowledged Prof. Fukuyama for his thoughtful discussions and expert guidance, which have been instrumental in shaping the direction and depth of this study.

Disclosure statement

No potential conflict of interest was reported by the author(s).

Funding

This work was supported by the Japan Science and Technology Agency (JST) CREST (Grant No. JPMJCR21O1). This work was partially supported by the Japan Society for the Promotion of Science (KAKENHI) Grant-in-Aid for Scientific Research (A) (21H04656).

ORCID

Daigo Furuya http://orcid.org/0000-0003-1558-665X
Yoshio Miura http://orcid.org/0000-0002-5605-5452
Takahiro Yamazaki http://orcid.org/0000-0003-0738-9373
Alexandre Lira Foggiatto http://orcid.org/0000-0003-2395-6438
Yuma Iwasaki http://orcid.org/0000-0002-7117-277X
Masato Kotsugi http://orcid.org/0000-0002-4841-1808

Data availability statement

The data that support the findings of this study are available from the corresponding author upon reasonable request.

References

[1] Ikeda S, Miura K, Yamamoto H, et al. A perpendicular-anisotropy CoFeB–MgO magnetic tunnel junction. Nat Mater. 2010;9(9):721–724. doi: 10.1038/nmat2804

[2] Yoda H, Kishi T, Nagase T, et al. High efficient spin transfer torque writing on perpendicular magnetic tunnel junctions for high density MRAMs. Curr Appl Phys. 2010;10(1):e87–e89. doi: 10.1016/j.cap.2009.12.021

[3] Kotsugi M, Maruyama H, Ishimatsu N, et al. Structural, magnetic and electronic state characterization of L10-type ordered FeNi alloy extracted from a natural meteorite. J Phys. 2014;26(6):064206.

[4] Miura Y, Ozaki S, Kuwahara Y, et al. The origin of perpendicular magneto-crystalline anisotropy in L10–FeNi under tetragonal distortion. J Phys. 2013;25(10):106005.

[5] Kojima T, Ogiwara M, Mizuguchi M, et al. Fe-Ni composition dependence of magnetic anisotropy in artificially fabricated L10-ordered FeNi films. J Phys. 2014;26(6):064207.

[6] Saito M, Ito H, Suzuki Y, et al. Fabrication of L10-FeNi by pulsed-laser deposition. Appl Phys Lett. 2019;114(7):072404.

[7] Ito H, Saito M, Miyamachi T, et al. Fabrication of L10-type FeCo ordered structure using a periodic Ni buffer layer. AIP Adv. 2019;9:045307.

[8] Matsui K, Kanamori K, Toyoura K, et al. Introduction to bayesian optimization and its application to material engineering. Materia Jpn. 2019;58(1):12–16.

[9] Ju S, Shiga T, Feng L, et al. Designing nanostructures for phonon transport via Bayesian optimization. Phys Rev X. 2017;7(2):021024.

[10] Tsuji Y, Yoshioka Y, Okazawa K, et al. Exploring metal nanocluster catalysts for ammonia synthesis using informatics methods: a concerted effort of bayesian optimization, swarm intelligence, and first-principles computation. ACS Omega. 2023;8 (33):30335–30348. doi: 10.1021/acsomega.3c03456

[11] Kurniawan I, Miura Y, Hono K. Machine learning study of highly spin-polarized heusler alloys at finite temperature. Phys Rev Mater. 2022;6(9): L091402. doi: 10.1103/PhysRevMaterials.6.L091402

[12] Iwasaki Y, Sawada R, Saitoh E, et al. Machine learning autonomous identification of magnetic alloys beyond the Slater-Pauling limit. Commun Mater. 2021;2 (1):31.

[13] Furuya D, Miyashita T, Miura Y, et al. Autonomous synthesis system integrating theoretical, informatics, and experimental approaches for large-magnetic-anisotropy materials. Sci Technol Adv Mater Meth. 2022;2(1):280–293.

[14] Iwasaki Y. Autonomous search for materials with high Curie temperature using ab initio calculations and machine learning. Sci Technol Adv Mater Meth. 2024;4(1):2399494.

[15] Seko A, Togo A, Hayashi H, et al. Prediction of low-thermal-conductivity compounds with first-principles anharmonic lattice-dynamics calculations and bayesian optimization. Phys Rev Lett. 2015;115(20):205901. doi: 10.1103/PhysRevLett.115.205901

[16] Yamashita T, Sato N, Kino H, et al. Crystal structure prediction accelerated by Bayesian optimization. Phys Rev Mater. 2018;2(1):013803.

[17] Tučs A, Berenger F, Yumoto A, et al. Quantum annealing designs nonhemolytic antimicrobial peptides in a discrete latent space. ACS Med Chem Lett. 2023;14(5):577–582.

[18] Iwasaki Y, Jaekyun H, Sakuraba Y, et al. Efficient autonomous material search method combining ab initio calculations, autoencoder, and multi-objective Bayesian optimization. Sci Technol Adv Mater. 2022;2(1):365–371. doi: 10.1080/27660400.2022.2123263

[19] Iwasaki Y, Toyama R, Yamazaki T, et al. Autonomous search for half-metallic materials with B2 structure. Sci Technol Adv Mater. 2024;4(1):2403966. doi: 10.1080/27660400.2024.2403966

[20] Kresse G, Hafner J. Ab initio molecular dynamics for liquid metals. Phys Rev B. 1993;47(1):558. doi: 10.1103/PhysRevB.47.558

[21] Kresse G, Furthmüller J. Efficiency of ab-initio total energy calculations for metals and semiconductors using a plane-wave basis set. Comput Mater Sci. 1996;6:15–50.

[22] Kresse G, Furthmüller J. Efficient iterative schemes for ab initio total-energy calculations using a plane-wave basis set. Phys Rev B. 1996;54(16):11169. doi: 10.1103/PhysRevB.54.11169

[23] Prayogo GI, Tirelli A, Utimula K, et al. SHRY: application of canonical augmentation to the atomic substitution problem. J Chem Inf Model. 2022;62 (12):2909–2915.

[24] Ong SP, Richards WD, Jain A, et al. Python materials genomics (pymatgen): a robust, open-source python library for materials analysis. Comput Mater Sci. 2013;68:314–319. doi: 10.1016/j.commatsci.2012.10.028

[25] Perdew JP, Burke K, Ernzerhof M. Generalized gradient approximation made simple. Phys Rev Lett. 1996;77(18):3865. doi: 10.1103/PhysRevLett.77.3865

[26] Blöchl PE. Projector augmented-wave method. Phys Rev B. 1994;50:17953.

[27] Monkhorst HJ, Pack JD. Special points for Brillonin-zone integrations. Phys Rev B. 1976;13:5188.

[28] Blöchl PE, Jepsen O, Andersen OK. Improved tetrahedron method for Brillouin-zone integrations. Phys Rev B. 1994;49(23):16223. doi: 10.1103/PhysRevB.49.16223

[29] Daalderop GHO, Kelly PJ, Schuurmans MFH. First-principles calculation of the magnetocrystalline anisotropy energy of iron, cobalt, and nickel. Phys Rev B. 1990;41(17):11919. doi: 10.1103/PhysRevB.41.11919

[30] Weinert M, Watson RE, Davenport JW. Total-energy differences and eigenvalue sums. Phys Rev B. 1985;32(4):2115. doi: 10.1103/PhysRevB.32.2115

[31] Ueno T, Rhone TD, Hou Z, et al. COMBO: an efficient bayesian optimization library for materials science. Mater Discov. 2016;4:18–21.

[32] Motoyama Y, Tamura R, Yoshimi K, et al. Bayesian optimization package: PHYSBO. Comput Phys

Commun. 2022;278:108405. doi: 10.1016/j.cpc.2022.108405
[33] Thompson WR. On the likelihood that one unknown probability exceeds another in view of the evidence of two samples. Biometrika. 1933;25(3–4):285–294. doi: 10.1093/biomet/25.3-4.285
[34] Jones DR, Schonlau M, Welch WJ. Efficient global optimization of expensive black-box functions. J Glob Optim. 1998;13:455–492.
[35] Kushner HJ. A new method of locating the maximum point of an arbitrary multipeak curve in the presence of noise. J Basic Eng. 1964;86:97–106.
[36] Couckuyt I, Deschrijver D, Dhaene T. Fast calculation of multiobjective probability of improvement and expected improvement criteria for pareto optimization. J Glob Optim. 2014;60(3):575–594.
[37] Ikebata H, Hongo K, Isomura T, et al. Bayesian molecular design with a chemical language model. J Comput Aided Mol Des. 2017;31(4):379–391.
[38] Wang Z, Hutter F, Zoghi M, et al. Bayesian optimization in a billion dimensions via random embeddings. Jair. 2016;55:361–387. doi: 10.1613/jair.4806
[39] Gulli A, Pal S. Deep learning with Keras. Birmingham, UK: Packt Publishing Ltd; 2017.
[40] Bruno P. Tight-binding approach to the orbital magnetic moment and magnetocrystalline anisotropy of transition-metal monolayers. Phys Rev B. 1989;39(1):865. doi: 10.1103/PhysRevB.39.865
[41] Okabayashi J, Miura Y, Munekata H. Anatomy of interfacial spin-orbit coupling in Co/Pd multilayers using X-ray magnetic circular dichroism and first-principles calculations. Sci Rep. 2018;8(1):8303. doi: 10.1038/s41598-018-26195-w
[42] Okabayashi J, Tanaka MA, Morishita M, et al. Origin of perpendicular magnetic anisotropy in CoxFe3-x O4+δ thin films studied by x-ray magnetic circular and linear dichroisms. Phys Rev B. 2022;105(13):134416.
[43] Burkert T, Nordström L, Eriksson O, et al. Giant magnetic anisotropy in tetragonal FeCo alloys. Phys Rev Lett. 2004;93(2):027203.
[44] Kota Y, Sakuma A. Degree of order dependence on magnetocrystalline anisotropy in body-centered tetragonal FeCo alloys. Appl Phys Express. 2012;5(11):113002. doi: 10.1143/APEX.5.113002
[45] Kota Y, Sakuma A. Theoretical verification of magnetic anisotropy in tetragonal Fe-co alloys. J Magn Soc Jpn. 2013;37:17–23.
[46] Aleksander AL, Nguyen MC, Wang CZ, et al. Concentration-tuned tetragonal strain in alloys: application to magnetic anisotropy of FeNi1-xCox. Phys Rev B. 2019;100(10):104429.
[47] Hasegawa T, Niibori T, Takemasa Y, et al. Stabilisation of tetragonal FeCo structure with high magnetic anisotropy by the addition of V and N elements. Sci Rep. 2019;9(1):5248. doi: 10.1038/s41598-019-41825-7
[48] Hasegawa T, Shirai C. Effect of V addition on the body-centered cubic to body-centered tetragonal to face-centered cubic structural transformation of N-containing Fe and FeCo films. Thin Solid Films. 2021;739:138990. doi: 10.1016/j.tsf.2021.138990